Telecommunications and Radio Engineering, 74 (20):1857-1869 (2015)

SCHUMANN RESONANCE FOR CONDUCTIVITY PROFILE OF ATMOSPHERE WITH SINGLE BENDING *

***Yu.P. Galuk*[1], *A.P. Nickolaenko*[2♦], *& M. Hayakawa* [3]**

[1]*Saint-Petersburg State University, 7/9 Universitetskaya nab., St. Petersburg, 199034, Russia*

[2]*A.Ya. Usikov Institute for Radiophysics and Electronics of the National Academy of Sciences of Ukraine 12, Academician Proskura St., Kharkiv 61085, Ukraine*

[3] *Hayakawa Institute of Seismo Electromagnetics Co. Ltd. UEC Incubation Center-508, 1-5-1 Chofugaoka, Chofu Tokyo 182-8585, Japan*

♦Address all correspondence to A.P. Nickolaenko E-mail: sasha@ire.kharkov.ua

Investigations remains update of relationship between the parameters of global electromagnetic (Schumann) resonance and characteristics of vertical profile of atmosphere conductivity. We use the rigorous full wave solution of the electrodynamic problem in the spherical Earth-ionosphere cavity and compare the results with the described in literature heuristic knee model having a single kink. By using parameters of this heuristic model, we constructed vertical profile of atmospheric conductivity and used it in the rigorous full wave solution for the propagation constant of ELF radio waves. Afterwards, the power spectra were computed of vertical electric and horizontal magnetic fields in the framework of the uniform global distribution of the planetary thunderstorm activity. We show that conductivity profile based on the one kink does not match the rigorous full wave solution and the subsequent computations of the power spectra of the Schumann resonance.

KEY WORDS: *Schumann resonance, atmospheric conductivity, full wave solution, knee model*

1. INTRODUCTION

Parameters of electromagnetic resonance in the Earth-ionosphere cavity depend on the atmosphere conductivity in the altitude range from 0 to 100 km. Solution of the electrodynamic problem in the cavity with a vertically non-uniform ionosphere might

* Originally published in *Radiophysics and Electronics*, Vol. 6(20), No 3, 2015, pp. 22–29.

be built in general case only by the numerical methods, one of which is the full wave solution (FWS) [1-5]. The inverse electrodynamic problem when we derive the vertical conductivity profile from the observed parameters of the global electromagnetic (Schumann) resonance has not been solved in the general formulation. Usually, a realistic profile is selected from direct solutions constructed for the set of models: the best fitting profile is chosen as corresponding to observations.

On the other hand, the height profile of atmospheric conductivity $\sigma(z)$ is not mandatory for computing the electromagnetic fields and interpretation of observations. It is sufficient to know the propagation constant of radio waves $\nu(f)$ and the effective height of the ionosphere above the ground, as these quantities are included in the standard formulae for the fields together with the source current moment and the source–observer distance [6,7]. The real profile $\sigma(z)$ is required when computing the unknown propagation constant and the effective ionosphere height. The simplified approach is often used when the height of the lower ionosphere boundary is accepted of 60 km, and the propagation constant is calculated by using observed peak frequencies and the quality factors of resonance peaks [1]. Thus, the standard or the reference model was obtained [8] for the propagation constant of extremely low frequencies (ELF 3–3000 Hz) radio waves. It summarizes substantial experimental data collected in observatories around the world. Other models are used in the frequency band of Schumann resonance along with the standard, and the simplest one is the linear dependence $\nu(f) = (f - 2)/6 - if/100$ [6,7]. This model was also based on observational data, and it is sufficiently accurate. It allowed to describe correctly the observed ELF pulsed waveforms of Q-bursts arriving from the distant powerful lightning strokes and to accurately derive the source–observer distance [9].

2. EXPONENTIAL MODEL

Kind of a breakthrough was made in paper [10] devoted to solving the radio propagation problem for monochromatic ELF signals. After extensive modeling, the authors suggested a method of approximate calculation of the propagation constant at a given frequency in the flat waveguide, provided that you know the vertical conductivity profile $\sigma(z)$. The idea was as follows.

1. The scale height dependence is constructed $\zeta(z)$ form the vertical profile $\sigma(z)$. That is, the $\sigma(z)$ dependence is approximated by appropriate exponential function in the vicinity of each height, and the local height scale $\zeta(z)$ is found for this exponent. Thus, the auxiliary profile is found of the height scale relevant to a given altitude profile of conductivity.

2. At a fixed frequency, two characteristic heights are derived together with the two scale heights by using functions $\sigma(z)$ and $\zeta(z)$. The conduction and the displacement currents are equal at the first, the lower height. Since fast decrease of the electric field amplitude begins above this height, it is called the "electric" height h_E Thus, two real parameters are found: the height h_E and the relevant scale height ζ_E.

3. The second characteristic height is found where the wavelength in the plasma medium becomes equal to the local scale high of conductivity profile. It was shown in [10] that magnetic field of the ELF radio wave penetrates up to this height, and the magnetic field amplitude begins to decrease rapidly above it. This characteristic height and the corresponding altitude scale were called "magnetic": h_M and ζ_M

4. According to [10], the phase velocity of ELF radio wave depends on the ratio h_M/h_E, and its attenuation factor is directly proportional to the sum $(\zeta_E/h_E + \zeta_M/h_M)$.

We will not overload our paper by equations, as a reader can easily find these in the cited literature.

Afterwards, the approach suggested in [10] was adopted for obtaining the propagation constant in the wide frequency band [11-15]. Various exponential conductivity profiles are described in literatures that provide realistic models of ELF propagation constant. Typical parameters of these profiles are: $h_E \approx 50$ km and $\zeta_E \approx 3$ km at the first Schumann resonance mode frequency $f = 8$ Hz (this value is regarded as reference frequency). The magnetic characteristic height is found from equation $h_M = h_E - 2\zeta_E\,(2k\zeta_E) \approx 95$ km. The scale height ζ_M is taken equal to ζ_E (single scale model), or some other value is ascribed to it (two-scale model), see e.g. [14].

It must be emphasized that approach described is just a convenient tool for estimating the ELF propagation constant. However, no difficulties are met when parameters are used of such an exponential model for constructing the corresponding function $\sigma(z)$. For example, one can easily build a conductivity profile in the vicinity of the lower characteristic height by using values: $f = 8$ Hz, $h_E = 50$ km, and $\zeta_E = 3$ km. This will be an exponent passing through the point $z = h_E = 50$ km where the air conductivity is equal to $\sigma_0 = 2\,\pi\,8\,\varepsilon_0 = 4.444\ 10^{-10}$ S/m (ε_0 is the permittivity of a vacuum), and the scale height $\zeta_E = 3$km. In the vicinity of the upper characteristic height of The graph passes through $h_M = h_E - 2\,\zeta_E \ln(2k\zeta_E) = 95.6$ km (k is the wave number the free space) and $\sigma_M(h_M) = [4\mu_0\,2\,\pi\,8\,\zeta_E^2]^{-1} = 4.4\cdot 10^{-4}$ S/m (μ_0 is the permeability of vacuum). Here, the curve $\sigma(z)$ has the scale height ζ_M. Obviously, such a profile looks as a broken straight line passing through these two points in the coordinates "height versus the logarithm of conductivity". However, until publication of paper [16], nobody applied such a profile in the rigorous full wave solution for obtaining the $v(f)$ function.

Several situations are possible for a conductivity profile derived from an exponential model

1. Lines drawn from the characteristic heights intersect at an intermediate height and form a kink or a "knee". This occurs when the lower scale height exceeds the upper one: $\zeta_E > \zeta_M$.

2. The knee is bent in the opposite direction when $\zeta_E < \zeta_M$. This situation occurs on the Saturnian moom Titan.

3. The kink might be missing, or the parallel upper and lower parts of the profile can not cross at all, or the might intersect at altitudes contradicting to a common sense.

Nevertheless, one can easily build an equivalent altitude dependence of the atmosphere conductivity $\sigma(z)$ by using parameters of an exponential model.

Obviously, one can use such a profile in the rigorous solution of the electrodynamic problem and check to what an extent the approximate solution [10] matches the exact one. Such a comparison was made in [16], where the exponential profile was used in constructing the rigorous full wave solution. It turned out that approximate formulas predict the real part of propagation constant Re[$\nu(f)$] with the accuracy of 1–2%. Concerning the imaginary part Im[$\nu(f)$] (the wave attenuation), the approximate value may deviate from the accurate one by 10–15%.

This finding attracted no significant attention, despite it means the following. Let us assume that by using works [11-15] we have chosen the model parameters that allow obtaining the experimental parameters of the Schumann resonance. Thus, the approximate solution is close to the experimental observations providing a "realistic profile". Simultaneously, the exact solution for the same profile obviously deviates from observations! Such a situation occurs when the electromagnetic resonance in the Earth-ionosphere cavity is directly simulated, for example, by using the finite dimension time domain (*FDTD*) method. The *FDTD* solution itself requires significant resources, and it is unacceptable when the above "approximately optimal" profile $\sigma(z)$ provides data noticeably deviating from observations. It is necessary to remember that an exponential model [10] is only a convenient interpretation, but it does not provide a description exactly corresponding to the real physical object.

3. KNEE MODEL

A further step in development of approximating heuristic models was the "knee model" [17]. It improved accuracy of description of the resonance quality factor. The model became popular, and its approximate nature was forgotten. In distinction from a two-scale model, the knee model operates with four frequency-dependent parameters. Two of them are interpreted as the height scales nearby the characteristic electric and magnetic heights. The other two are the characteristic heights being the complex functions of frequency. The propagation constant $\nu(f)$, which is used in the calculation of the fields, is computed using the model parameters.

Distinctions of the knee model from the two-scale exponential model is that the magnetic height is separately introduced in addition to the two scale heights in the vicinity of electric height. At the first Schumann resonance frequency the lower (the greater) scale height plays the dominant role. At the higher modes, the transition occurs to the upper (smaller) scale height. Frequency variations of all elements included in the formula allow for more accurate description of the modal quality factors as function of the number.

Parameters of the knee model [17] were verbally referred to a certain conductivity profile, however, authors never showed such a profile. Only paper [18] presented the lower part of the knee profile in the vicinity of electric height, which were compared with the aeronomy data. Since none of the works operating with the knee model has constructed the relevant dependence $\sigma(h)$, while the direct numerical solution of the

problem using the grid technique applies the altitude profile of air conductivity, the authors of relevant works had to invent such profiles by themselves of [19-23]. The resonance frequencies obtained in the direct simulations usually deviate from those values predicted by the "same" knee model. We analyze such deviations and demonstrate that they always exist and are conditioned by the approximate nature of the model itself.

In works applying direct modeling [20-23], the conductivity profile were used bent in the vicinity of 50 – 60 km, which is rather close to the real situation around the lower characteristic height of Re[h_e]. Simultaneously, presence was ignored of a separately introduced upper characteristic height h_M and the scale height ζ_M. Thus the conductivity profiles were obtained and applied in computations with a single kink. It is obvious that under these conditions, obtaining data corresponding to observations depends solely on the authors' luck.

The exponential model profiles of conductivity having a single bending were widely used in computations of the Schumann resonance [6,7,14,15]. These are usually regarded as the two-scale model [14]. Thus, application of such model in the grid technique inadvertently returns a researcher to the old-fashion two-scale profile, as the separately postulated upper characteristic height is excluded from the model.

4. CONDUCTIVITY PROFILE, PROPAGATION CONSTANT, AND POWER SPECTRA

Let us build the $\sigma(h)$ profile corresponding to the knee model, as obtaining of such a profile was not presented in literature. The knee model operates by two complex characteristic heights $h_E(f)$ and $h_M(f)$ together with two real (with zero imaginary part) scale heights $\zeta_E(f)$ andζ_M (f) in the neighborhood of these heights. All listed values depend on frequency, and it is possible to calculate the propagation constant with the help of equations of [17]. It is unclear though, in what a way one can construct the real profile $\sigma(h)$ independent of frequency by using the four above listed functions of frequency.

We use here the results of work [18], where authors of the knee model [17] analyze in detail the behavior of the air conductivity in the knee area and compare it with the aeronomy data. An example of the classic $\sigma(h)$ profile was taken from [24], and it is shown by curve 1 in Fig. 1. Curves 2 and 3 in this figure demonstrate altitude variations of the conductivity in the day and night ionosphere, adopted from [18]. Here, the abscissa depicts the logarithm of air conductivity and the ordinate shows the height above the ground surface.

Bending of the curves 2 and 3 in Fig. 1 is physically explained by alteration of the prevailing charge carriers. At lower altitudes, the air conductivity is supported by ions and ion complexes. It varies relatively slowly along the vertical direction. At higher altitudes, the mobile free electrons dominate, their concentration rapidly increases with altitude, and the conductivity of the medium increases rather fast. To avoid confusion, we use in what follows the word combination "transition from ionic to electronic

conductivity" or abbreviation TIE instead of the terms: "knee" or the "two-scale model". The term TIE refers only to a specific type of profile [18] discussed below. Similar profiles were applied in the *FDTD* solutions [20-23], so that we will try to establish to what an extent the model data thus obtained correspond to reality.

A TIE profile allows for accurate computing of the frequency dependence of the ELF radio wave propagation constant. Afterwards, the power spectra of the fields might be computed in the Schumann resonance frequency band. Instead of the curves 2 and 3 shown in Fig. 1, we use a family of conductivity profiles having the transition from ionic to electron conductivity at varying altitude. This family is shown in Fig. 2.

The ion to electron transition is described by the two exponential functions of altitude having different scale heights. All quantities were taken from [18]. The height variation of air conductivity in the bottom region is conditioned by dominance of ions and ion complexes it is equal to:

$$\sigma_i(z) = \sigma_0 \left\{ \exp\left[\left(z - h_R \right) / \zeta_i \right] \right\}. \tag{1}$$

$\sigma_i(z)$ is the ionic conductivity, z is the altitude over the ground surface, $h_R = 1$ km is the reference height of ionic conductivity, $\sigma_0 = 9.1 \cdot 10^{-13}$ S/m is the ionic conductivity of atmosphere at the reference height, $\zeta_i = 10.7$ km is the scale height of vertical profile in the area where ions prevail [18].

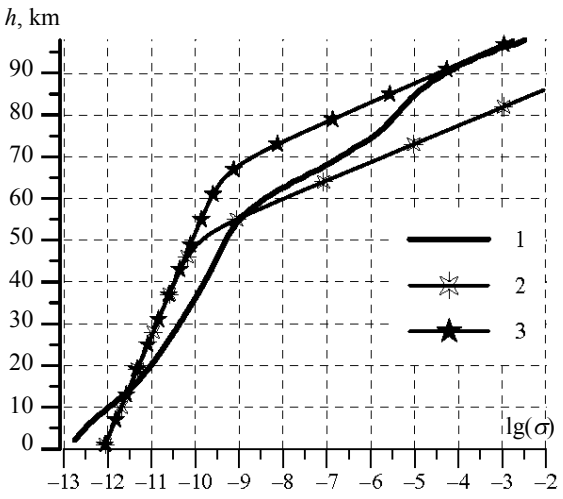

FIG. 1: Height profiles of air conductivity: curve 1 is the classical profile [24], curves 2 and 3 are the TIE functions for the ambient day and night conditions [18]

Free electrons dominate from the altitude h_T. Here, a new scale height appears:

$$\sigma_e(h) = \sigma_i(h) \exp\left[\left(z - h_T \right) / \zeta_e \right], \tag{2}$$

where σ_e is the electron conductivity, h_T is the transition altitude, $\zeta_e = 2$ km is the scale height of electron conductivity.

Atmospheric conductivity at a given altitude is equal to the sum of the ion and electron conductivities:

$$\sigma(h) = \sigma_i(h) + \sigma_e(h). \tag{3}$$

Figure 2 shows the bent altitude profiles $\sigma(h)$ in the interval $1 \le z \le 100$ km built for the model with all fixed parameters except the transition altitude h_T. This last varies from 34 (lower curve) to 70 km (upper curve) with the 4 km step. Plots in Fig. 2 show that conductivity varies relatively slowly with altitude in the interval of ion dominance. Above the transition, electrons play a major role, and conductivity increases rapidly with height here. Transition itself is described by a smoothly bent curve. All profiles are coincident in the area where ionic conductivity prevails. The upper parts of the curves corresponding to the area of electron conductivity form the vertically spaced "parallel" lines. Electrons start dominating in progressively higher area when h_T increases. Obviously, the lower profiles in Fig. 2 are close to the daytime ionosphere, and the upper profiles correspond to ambient night conditions.

We used the full wave solution [2–5] for computing the $\nu(f)$ propagation constant for each profile, and afterwards, we constructed the power spectra of the Schumann resonance in the vertical electric and horizontal magnetic fields.

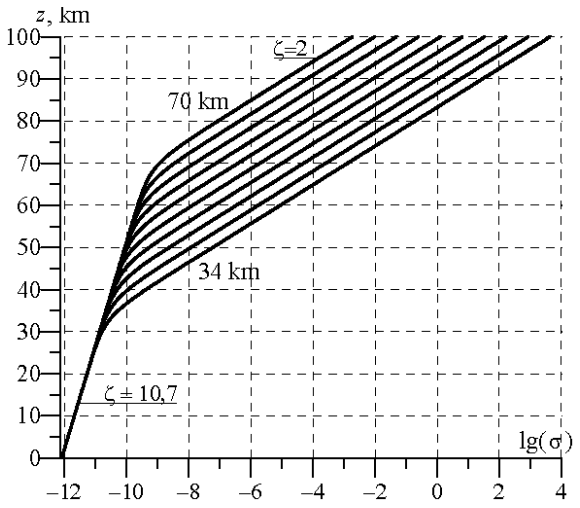

FIG. 2: Profiles with ion to electron transition at different altitudes

The lightning strokes serving as the source of the field were assumed to be uniformly distributed over the entire globe. This allowed us to avoid the dependence of spectral pattern on the source distance. The spectrum of the source current moment was independent of frequency and equal to 1. The random lightning strokes are

independent of each other, and their succession forms a Poisson pulsed process. This is why the resulting power spectrum is the sum of individual power spectra of events.

Power spectrum of the vertical electric field might be found in three different ways. The first one is computing of the following series [6,7]:

$$\left\langle \left|E(f)\right|^2 \right\rangle \approx \left|\frac{\nu(\nu+1)}{\omega}\right|^2 \sum_{n=0}^{\infty} \frac{2n+1}{\left|n(n+1)-\nu(\nu+1)\right|^2}. \tag{4}$$

Here, ν is the propagation constant of ELF radio waves, ω is the circular frequency, $n = 0, 1, 2$, etc. is the mode number.

Equation (4) is obtained by integrating the field expansion into the zonal harmonic series with the uniform distribution of field sources over the Earth's surface [6, 7]. Unfortunately, a similar formula cannot be deduced for the horizontal magnetic field owing to its substantial (non-integrable) singularity at the field source. Therefore, we used either the numerical integration by the Monte Carlo method or the direct computation of integral over the entire Earth's surface except a small vicinity of the source. The result computed by using formula (4) served as a reference for evaluating the accuracy of the Monte Carlo and the direct numerical integration. Deviations in the resulting magnitude of the power spectra did not exceed the ± 3% level, which is quite sufficient.

The second way of computations exploits the Monte Carlo method. The power spectra are calculated as the following sums:

$$<\left|E(f)\right|^2> = \frac{|\nu(\nu+1)|^2}{\omega^2} \times \sum_M \sin\theta_k \left|\frac{P_\nu\left[\cos(\pi-\theta_k)\right]}{\sin(\nu\pi)}\right|^2; \tag{5}$$

and

$$<\left|H(f)\right|^2> = \sum_M \sin\theta_k \cos^2\varphi_k \left|\frac{\frac{d}{d\theta}P_\nu\left[\cos(\pi-\theta_k)\right]}{\sin(\nu\pi)}\right|^2, \tag{6}$$

where M is the number of tests, θ_k is the angular distance from the observer to the k-th lightning stroke (a random variable distributed uniformly in the interval $0 < \theta_k \le \pi$), the factor $\cos\varphi_k$ accounts for the distribution of the arrival azimuths (a random variable uniformly distributed in the range $0 < \varphi_k \le 2\pi$), the factor $\sin\theta_k$ accounts for the different length of the parallels. The number of tests in the Monte Carlo algorithm was chosen $M = 2000$.

The third method exploited averaging of the individual power spectra over the random coordinates of lightning strokes, which is reduced to computation of sums similar to (5) and (6):

$$<|E(f)|^2>=\frac{|\nu(\nu+1)|^2}{\omega^2}\times\int_{\delta}^{\pi}\sin\theta\left|\frac{P_\nu\left[\cos(\pi-\theta)\right]}{\sin(\nu\pi)}\right|^2 d\theta; \qquad (7)$$

and

$$<|H(f)|^2>=\frac{1}{2}\int_{\delta}^{\pi}\sin\theta\left|\frac{\frac{d}{d\theta}P_\nu\left[\cos(\pi-\theta)\right]}{\sin(\nu\pi)}\right|^2 d\theta. \qquad (8)$$

Integrals (7) and (8) were computed by the Simpson (Cotes) method. As we noted before, the difficulty arises when computing the power spectrum of the magnetic field. The reason is that the Legendre function has a logarithmic singularity when θ is small (the source vicinity), and its derivative varies as $(\theta)^{-1}$. Therefore integral of the magnetic field intensity diverges in spite of the factor $\sin\theta$ in equations (6) and (8). The singularity is significant at distance of order of the ionosphere height. The easiest way to avoid it is integration of (6) and (8) starting from distances exceeding 200 km from the source, or from $\delta=\pi/10$. The argumentation is valid for the Monte Carlo and Simpson method.

After conducting statistical tests in the framework of the Monte Carlo procedure we obtain the spectrum for a conductivity profile for the given transition height h_T. Then, this parameter was changed, and computations repeated. The height h_T varied from 44 to 66 km with the step of 2 km. Thus, the power spectra were obtained of the both field components for each profile of the family shown in Fig. 2 by using the Monte Carlo method. The results are presented in Fig. 3 in the form of 2D maps built over the "frequency – transition height" plane. Such presentation combines individual spectra corresponding to different transition heights into the 2D survey of global electromagnetic resonance.

Figure 3(a) shows the profile of the power spectra of the horizontal magnetic field, and Fig. 3(b) depicts the vertical electric field data. The abscissa shows the frequency ranging from 1 to 25 Hz. The vertical axis shows the height h_T of the ion-electron transition. Resonance intensity is shown in arbitrary units by the dark inking, and the lines are given of the constant levels of the field intensity.

The first, second, and the third peaks are clearly seen in the relief of the Schumann resonance (dark areas). Maps of electric and magnetic fields have similar outline for the uniform source distribution. The resonance frequencies obviously increase with raising the transition height h_T. However, this dependence is weak: the shift of the first resonance peak does not exceed 0.2 Hz within the 44–66 km height range.

We evaluated the impact of TIE height on the power spectra by using the set of resonance patterns relevant to different transition heights h_T. Results of computations might indicate what a profile matches the observed frequencies of 7.8-8.0, 13.8-14.0, 9.8-20.0 Hz etc. in the best way. Such a profile could be recommended for the further time-consuming simulation of the Schumann resonance by using the *FDTD* technique. The graphs of Fig. 3 demonstrate that none of the TIE models is appropriate for the

direct modeling. The fact is that none of the profiles provides realistic values of the resonant frequencies: all of them exceed the experimentally observed values. Even the lowest transition altitude $h_T = 44$ km provides the first peak frequency of 8.3 Hz, which is significantly higher than the observed values. Thus, data of paper [18] lead to the systematic errors in the ELF propagation constant in spite their solid background. Any of these profiles will lead to unrealistic resonant frequencies when applied in the *FDTD* modeling.

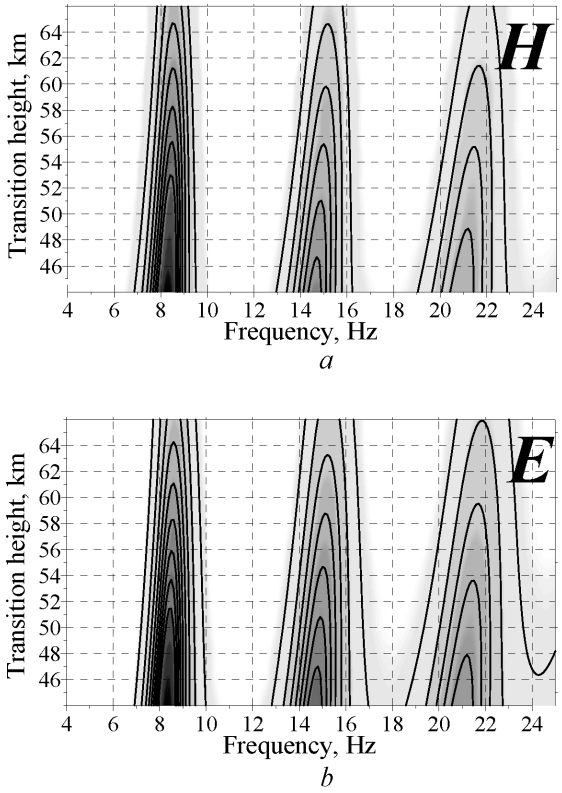

FIG. 3: Power spectra for the TIE model over frequency-transition altitude plane for thunderstorms infirmly covering the surface of the Earth: a) power spectra of the horizontal magnetic field; b) power spectra of the vertical electric field

Plots in Fig. 4 explain that the noted deviations in the peak frequencies of the power spectra are caused by the propagation constant of ELF radio waves. This figure contains the 2D profiles of real and imaginary parts of the propagation constant over the "frequency – transition height" plane. The plots in Fig. 4 are made similarly to Fig. 3; however, instead of the power spectra the lines are shown of the constant levels of the propagation constant. The top panel of this figure shows changes of the real part. The numbered lines correspond to the constant levels $\mathrm{Re}[\nu(f, h_T)] = n$ where n is the

resonance mode number. When comparing Figs. 3 and 4, we readily see that maxima of the power spectra in Fig. 3 correspond to lines Re[ν] = n in Fig. 4(a). Plot of Fig. 4(a) shows that conductivity profiles with the single kink [18] may provide a realistic value of the resonance frequency of 8 Hz when the transition height $h_T \leq 30$ km. This definitely contradicts the physical reality.

Application is inappropriate of the conductivity profile having a single kink in the direct electromagnetic simulations. At any rate, it does not provide the realistic peak frequencies in the power spectra. One of the reasons is that the knee model [17] additionally introduces the upper (magnetic) characteristic height and the relevant scale height. This was not done in the model [18], and the magnetic height appeared "automatically", similarly to the ordinary two-scale height model. Apparently, this leads to deviations in the power spectra. Thus, either model [18] requires further elaboration or more realistic $\sigma(h)$ functions should be used in the direct field computations. For example, the models might be used accounting for measurements of the fair weather fields in the global electric circuit [25-28].

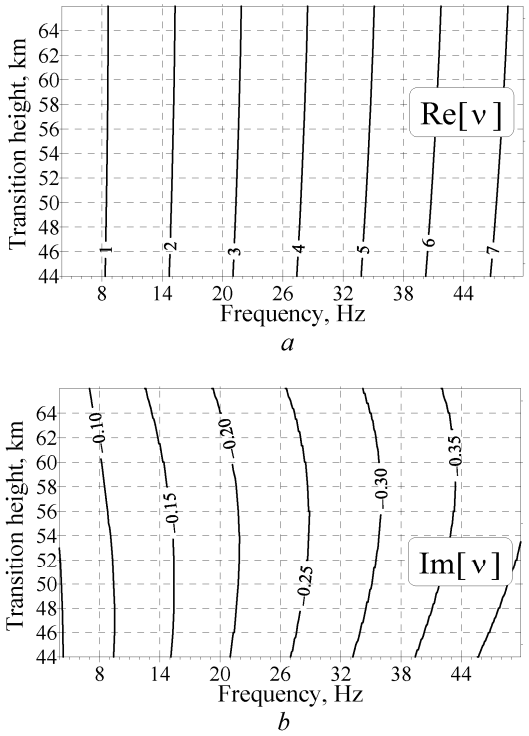

FIG. 4: Real (a) and imaginary (b) parts of ELF propagation constant in the TIE model

Figure 4(b) demonstrates another important feature of the TIE profile: the non-monotonic variations of the attenuation factor with alterations of the transition height.

It is especially noticeable at the higher resonance modes. The obvious maximum in the wave attenuation around $h_T = 50 \div 60$ km cannot be explained by elementary physical considerations, however, its presence might be important in the ELF radio propagation.

5. CONCLUSIONS

The above analysis shows that similarly to the exponential model [10], the simplified methods of calculating the propagation constant of ELF radio waves with the knee model do not allow constructing realistic vertical profiles of atmospheric conductivity. This impedes their application in the direct methods of field computations. In particular, the analyzed in detail model [18] does not withstand comparison with the rigorous full wave solution and the subsequent computations of the power spectra of the Schumann resonance.

The reason is that the TIE profile [18] is coincident with the two-scale exponential model [14]. Distinctions of these models might be found only in the magnitude of particular parameters. All knee models [17,19] separately introduce the upper (magnetic) characteristic height for consistency with the experimental observations. Thus, the number of model free parameters increases and the postulated magnetic height lies above the values found from the $h_M > h_E - 2\zeta_E \ln(2k\zeta_E)$ [14] and simultaneously $\zeta_M > \zeta_a$. This modification returns the computed peak frequencies and the quality factors of the Schumann resonance to the observed values.

Using would be reasonable of more realistic conductivity profiles in the laborious direct computations of electromagnetic fields. For instance, the profiles already tested in the adjacent frequency bands [25-28]. It might occur that some profiles published in literature do not match observations of the global electromagnetic resonance. Thus, computations by the full wave solution and the subsequent comparison of resonance spectra allows for chosing a realistic vertical profiles of the atmospheric conductivity.

REFERENCES

1. Bliokh, P.V., Nickolaenko, A.P., and Filippov, Yu.F., (1980), *Schumann resonances in the Earth–ionosphere cavity*, Peter Perigrinus, New York, - 168 p.
2. Hynninen, E.M. and Galuk, Yu.P., (1972), Field of vertical dipole over the spherical Earth with non-uniform along height ionosphere, *Problems of diffraction and radio wave propagation*. 11:109–120 (in Russian).
3. Bliokh, P.V., Galuk, Yu.P., Hynninen, E.M., Nickolaenko, A.P. et al., (1977), On the resonance phenomena in the Earth-ionosphere cavity, *Radiophysics and Quantum Electronics*. **20**(4):339–345, doi:10.1007/BF01033918 (in Russian).
4. Galuk, Yu.P. and Ivanov, V.I., (1978), Deducing the propagation charactericics of VLF fields in the cavity Earth–non-uinform along the height anisotropic ionosphere, *Problems of diffraction and radio wave propagation.* 16:148–153 (in Russian).
5. Galuk, Yu.P., Nickolaenko, A.P., and Hayakawa, M., (2015), Comparison of exact and approximate solutions of the Schumann resonance problem for the knee conductivity profile, *Telecommunications and Radio Engineering*, **74**(15):1377-1390.

6. Nickolaenko, A.P. and Hayakawa, M., (2002), *Resonances in the Earth-ionosphere cavity*, Dordrecht-Boston-L.: Kluwer Academic Publ., – 380 p.
7. Nickolaenko, A. and Hayakawa, M., (2014), *Schumann resonance for tyros (Essentials of Global Electromagnetic Resonance in the Earth–Ionosphere Cavity)*, Tokyo-Heidelberg-N. Y.-Dordrecht-L.: Springer, 2014. – Ser. XI. Springer Geophysics. – 348 p.
8. Ishaq, M. and Jones, D.Ll., (1977), Method of obtaining radiowave propagation parameters for the Earth–ionosphere duct at ELF, *Electronic Lett*. **13**(2):254–255.
9. Nickolaenko, A.P, Hayakawa, M., Ogawa, T., and Komatsu, M., (2008), Q-bursts: A comparison of experimental and computed ELF waveforms, *Radio Sci*. **43**(4):RS4014 (9 p.).
10. Greifinger, C. and Greifinger, P., (1978), Approximate method for determining ELF eigenvalues in the Earth–ionopshere waveguide, *Radio Sci*. **13**(5):831–837.
11. Nickolaenko, A.P. and Rabinowicz, L.M., (1982), On a possibility of global electromagnetic resonances at the planets of Solar system, *Kosmicheskie Issled*. **20**(1):82–89 (in Russian).
12. Nickolaenko, A.P. and Rabinowicz, L.M., (1987), On applicability of ELF global resonances for studing thunderstorm activity at Venus, *Kosmicheskie Issled.* **25**(2):301–306 (in Russian).
13. Sentman, D.D., (1990), Approximate Schumann resonance parameters for a two-scale-height ionosphere, *J. Atmos. Terr. Phys*. **52**(1):35–46.
14. Sentman, D.D., (1995), Schumann Resonances, in: *Handbook of Atmospheric Electrodynamics: Vol. 1*, L.-Tokyo: CRC Press, Boca Raton, pp. 267−298.
15. Füllekrug, M., (2000), Dispersion relation for spherical electromagnetic resonances in the atmosphere, *Phys. Lett. A*. **275**(1–2):80–89.
16. Jones, D.Ll. and Knott, M., (2003), Computations of electromagnetic resonance in the Earth–ionosphere cavity by the full wave solution and the approximate model, *Radio Physics and Electronics*. **8**(1):55–66 (in Russian).
17. Mushtak, V.C. and Williams, E., (2002), Propagation parameters for uniform models of the Earth-ionosphere waveguide, *J. Atmos. Solar-Terr. Phys*. **64**(6):1989–2001.
18. Greifinger, P.S., Mushtak, V.C., and Williams, E.R., (2007), On modeling the lower characteristic ELF altitude from aeronomical data, *Radio Sci*. **42**(2):RS2S12 (12 p.).
19. Pechony, O. and Price, C., (2004), Schumann resonance parameters calculated with a partially uniform knee model on Earth, Venus, Mars, and Titan, *Radio Sci*. **39**(5):RS5007 (10 p.).
20. Yang, H. and Pasko, V.P., (2005), Three-dimensional finite-difference time domain modeling of the Earth-ionosphere cavity resonances, *Geophys. Res. Lett*. **32**(3):L03114 (4 p.).
21. Morente, J.A., Molina-Cuberos, G.J., Porti, J.A. et al., (2003), A numerical simulation of Earth's electromagnetic cavity with the Transmission Line Matrix method: Schumann resonances, *J. Geophys. Res*. **108**(A5):SIA 17-1–17-11.
22. Toledo-Redondo, S., Salinas, A., Morente-Molinera, J.A. et al., (2013), Parallel 3D-TLM algorithm for simulation of the Earth-ionosphere cavity, *J. Computational Phys*. **236**(3):367–379.
23. Zhou, H., Yu, H., Cao, B., Qiao, X., (2013), Diurnal and seasonal variations in the Schumann resonance parameters observed at Chinese observatories, *J. Atmos. Solar-Terr. Phys*. **98**(1):86–96.
24. Cole, R.K. and Pierce, E.T., (1965), Electrification in the Earth's atmosphere from altitudes between 0 and 100 kilometers, *J. Geophys. Res*. **70**(11):2735–2749.
25. Makino, M. and Ogawa, T., (1984), Response of atmospheric electric field and air-earth current to variations of conductivity profiles, *J. Atmos. Solar-Terr. Phys*. **46**(5):431–435.
26. Ogawa, T., (1985), Fair Weather Field Electricity, *J. Geophys. Res*. **90**(4D):5951–5961
27. Rycroft, M.J., Odzimek, A., Arnold, N.F. et al., (2007), New model simulations of the global atmospheric electric circuit driven by thunderstorms and electrified shower clouds: The roles of lightning and sprites, *J. Atmos. Solar-Terr. Phys*. **69**(17–18):2485–2509.
28. Rycroft, M.J., Nicoll, K.A., Aplin, K.L., and Harrison, R.G., (2012), Recent advances in global electric circuit coupling between the space environment and the troposphere, *J. Atmos. Solar-Terr. Phys*. **90-91**:198–211.